Novel variants in *STAG2* and *PKD1* associate with multiple congenital malformations and autosomal dominant polycystic kidney disease in a Chinese family: A case report and literature review

QI YANG[1-3*], QIANG ZHANG[1-3*], SHENG YI[1-3], XUNZHAO ZHOU[1-3], YIYAN RUAN[4], SHUJIE ZHANG[1-3], SHANG YI[1-,3], QINLE ZHANG[1-3], ZAILNG QIN[1-3] and JINGSI LUO[1-3,4]

[1]Guangxi Key Laboratory of Reproductive Health and Birth Defects Prevention, Maternal and Child Health Hospital of Guangxi Zhuang Autonomous Region, Nanning, Guangxi Zhuang Autonomous Region 530023, P.R. China; [2]Department of Genetic and Metabolic Central Laboratory, Maternal and Child Health Hospital of Guangxi Zhuang Autonomous Region, Nanning, Guangxi Zhuang Autonomous Region 530023, P.R. China; [3]Guangxi Clinical Research Center for Birth Defects, Maternal and Child Health Hospital of Guangxi Zhuang Autonomous Region, Nanning, Guangxi Zhuang Autonomous Region 530023, P.R. China; [4]Department of Pediatric Neurology, Guangxi Clinical Research Center for Pediatric Diseases, Maternal and Child Health Hospital of Guangxi Zhuang Autonomous Region, Nanning, Guangxi Zhuang Autonomous Region 530023, P.R. China

Received June 6, 2025; Accepted November 14, 2025

DOI: 10.3892/etm.2025.13057

Abstract. Cohesinopathies are rare multisystem disorders caused by defects in the cohesin complex, which is critical for chromosome segregation, DNA repair, replication, heterochromatin formation and gene transcription regulation. Stromal antigen 2 (STAG2), a key cohesin component, is linked to neurodevelopmental disorders such as X-linked holoprosencephaly 13 and Mullegama-Klein-Martinez syndrome (MKMS). Polycystic kidney disease (PKD), particularly autosomal dominant PKD (ADPKD), is characterized by renal cysts and is commonly associated with variants in the *PKD1* gene. In the present study, a Chinese family was enrolled, which included an infant diagnosed with MKMS and familial PKD. Trio whole-exome sequencing (trio-WES) was performed to identify a heterozygous in-frame deletion variant in *STAG2* [NM_001042750.2:c.1775_1777del, p.(Pro592del)] and a heterozygous frameshift variant in *PKD1* [NM_001009944.3:c.8985delC, p.(Ser2996fs*78)] in the proband. The *STAG2* variant [c.1775_1777del, p.(Pro592del)] was confirmed by Sanger sequencing to be absent in other family members and was therefore *de novo*. By contrast, the *PKD1* variant [c.8985delC, p.(Ser2996fs*78)] was identified in the mother, aunt and grandmother of the proband. The proband exhibited clinical features consistent with *STAG2*-related disorders, including seizures, global developmental delay, short stature, microcephaly, hypotonia, dysmorphic features, incomplete cleft palate, micrognathia, spina bifida occulta and duplication of the middle phalanx of the third finger on the left hand. Comparative analysis of the present patient and previously reported cases with *STAG2* variants suggested that intellectual disability, brain abnormalities, dysmorphic features and skeletal anomalies are the core clinical features of *STAG2*-related disorders. Furthermore, familial PKD was observed in the proband, mother, aunt and grandmother, confirming an autosomal dominant inheritance pattern associated with the *PKD1* variant. In summary, the present report identified a novel *de novo STAG2* variant associated with multisystem congenital malformations and a novel familial *PKD1* variant causing ADPKD, expanding the genetic and phenotypic spectrum of these disorders. The present findings highlight the utility of WES in diagnosing complex genetic conditions.

Correspondence to: Professor Jingsi Luo, Guangxi Key Laboratory of Reproductive Health and Birth Defects Prevention, Maternal and Child Health Hospital of Guangxi Zhuang Autonomous Region, 59 Xiangzhu Road, Nanning, Guangxi Zhuang Autonomous Region 530023, P.R. China
E-mail: yangqisklmg126@126.com

*Contributed equally

Key words: trio whole-exome sequencing, *STAG2* gene, *STAG2*-related disorders, novel variant, *PKD1* gene, polycystic kidney disease

Introduction

Cohesinopathies are a group of rare diseases caused by defects in the cohesin complex. These disorders involve multiple organ systems, including the brain, heart and skeleton, and stem from impairments in fundamental cellular processes such as chromosome segregation, DNA repair, DNA replication, heterochromatin formation and gene transcription (1). The cohesin complex, an evolutionarily conserved large functional

unit, consists of four core proteins, structural maintenance of chromosomes (SMC) protein 1A, SMC2, RAD21 and stromal antigen (STAG)1/2. Additionally, several regulatory proteins associated with this complex have been implicated in a wide range of human diseases (2). The *STAG2* gene (Online Mendelian Inheritance in Man 300826, NM_001042751), located on chromosome Xq25, comprises 34 exons and encodes the STAG2 cohesin complex component, which is involved in gene expression, DNA repair and genomic integrity (3). Variants in *STAG2* have been identified as the causative factor for neurodevelopmental disorders, such as X-linked holoprosencephaly 13 (HPE13) and Mullegama-Klein-Martinez syndrome (MKMS) (4). Patients with *STAG2* variants typically exhibit a wide range of phenotypic abnormalities, including intellectual disability, developmental delay, microcephaly, dysmorphic features, short stature, growth restriction, language impairment, delayed puberty, microtia, hearing loss and congenital heart and skeletal defects (5). At present, 19 *STAG2* variants have been reported in patients with HPE13 or MKMS (4-13). These include five missense variants, eight nonsense variants, five frameshift variants and one splice variant. Additional research is needed to elucidate the genotype-phenotype associations and underlying mechanisms of *STAG2*-related disorders.

Polycystic kidney disease (PKD) is a genetic disorder characterized by the formation of numerous cysts in the kidneys, leading to progressive kidney damage and eventual renal failure (14). The *PKD1* gene, located on chromosome 16, encodes polycystin-1, a large transmembrane protein involved in cell signaling, calcium ion regulation and the maintenance of normal renal tubular epithelial cell function (15). Variants in the *PKD1* gene disrupt polycystin-1 function, resulting in abnormal cell proliferation and the formation of fluid-filled cysts (16). These cysts gradually enlarge, compressing and replacing normal kidney tissue, thereby impairing kidney function (17). *PKD1* variants are responsible for most cases of autosomal dominant PKD (ADPKD), which is the most common form of PKD (18).

In the present report, a novel *de novo* heterozygous *STAG2* variant [NM_001042750.2:c.1775_1777del, p.(Pro592del)] and a novel heterozygous frameshift *PKD1* variant [NM_001009944.3:c.8985delC, p.(Ser2996fs*78)] were identified in a Chinese infant diagnosed with MKMS and familial PKD. Furthermore, through a comprehensive review of the literature, the genotypic, phenotypic and clinical features of STAG2-related disorders were summarized.

Case report

Patients and methods

Patients. In June 2024, a Chinese family with a member presenting seizures and developmental delays was referred to the Department of Pediatric Neurology of Maternal and Child Health Hospital of Guangxi Zhuang Autonomous Region (Nanning, China) for genetic evaluation. The study protocol was approved by the Ethics Committee of Maternal and Child Health Hospital of Guangxi Zhuang Autonomous Region (approval no. METc 2017-2-11) and conducted in accordance with the principles of The Declaration of Helsinki. Written informed consent was obtained from the patients and/or the parents of the affected individual for the publication of clinical data and images.

Whole-exome sequencing (WES) and Sanger validation. WES and Sanger validation were performed on genomic DNA extracted from 2 ml peripheral blood lymphocytes of the proband and available family members with the Lab-Aid DNA kit (cat. no. 604016; Xiamen Zeesan Biotech Co., Ltd.). DNA integrity was verified on a 1% agarose gel (≥20 kb high-molecular-weight band) and quantified by a Qubit dsDNA BR Assay (cat. no. Q32853; Thermo Fisher Scientific, Inc.). Trio-WES was carried out for the proband and parents: 3 μg of each DNA sample were sheared to 180-250 bp, end-repaired, A-tailed and ligated to Illumina-compatible adapters. Exome enrichment was performed with the Agilent SureSelect Human All Exon V5 capture kit (cat. no. 5190-6210; Agilent Technologies, Inc.). Captured libraries were pooled equimolarly, and the 280-320 bp insert size was confirmed on an Agilent High-Sensitivity DNA chip (Agilent Technologies, Inc.) run on the 2100 Bioanalyzer (cat. no. 5067-4626; Agilent Technologies, Inc.). Post-ligation Illumina NGS libraries served as the DNA source; their concentration was measured by SYBR Green I qPCR with the KAPA Library Quantification kit (Roche Diagnostics) using primers P5, 5'-AATGATACGGCGACCACCGA-3', and P7, 5'-CAAGCAGAAGACGGCATACGA-3', and a six-point kit-supplied linearized standard series (20-0.0002 pM). Reactions (20 μl) were run on a CFX96 (Bio-Rad Laboratories, Inc.) at 95˚C for 5 min, followed by 35 cycles of 95˚C for 30 sec and 60˚C for 45 sec, and finally a 65-97˚C melt curve. Unknown libraries were quantified by interpolation from the standard curve, diluted to 2 nM, denatured with 0.2 N NaOH and loaded at 10 pM onto an Illumina HiSeq 2000 flow-cell together with 1% PhiX control (cat. no. FC-110-3001; Illumina, Inc.). Sequencing was performed with the HiSeq 2000 Rapid SBS Kit v2, 100-cycle paired-end (cat. no. FC-402-4021; Illumina, Inc.) to generate 100-bp paired-end reads. Raw reads were aligned to the hg19/GRCh38 human reference genome with BWA-MEM (v0.7.15; https://github.com/lh3/bwa), and variant calling was completed using the Genome Analysis Toolkit (GATK v3.4; Broad Institute) following the best-practice workflow. Variant calling and annotation were performed using LifeMap TGex Version 3.0 (https://auth.shanyint.com/; customised website), with a focus on variants exhibiting a minor allele frequency of ≤0.001 in public databases, including the 1000 Genomes Project (https://www.internationalgenome.org/data), Exome Sequencing Project (http://evs.gs.washington.edu/EVS/) and Exome Aggregation Consortium (http://exac.broadinstitute.org).

The functional impact of candidate variants was predicted using *in silico* tools, including REVEL (https://sites.google.com/site/revelgenomics/), PolyPhen-2 (http://genetics.bwh.harvard.edu/pph2/), Sorting Intolerant From Tolerant (https://sift.bii.a-star.edu.sg/), Combined Annotation Dependent Depletion (https://cadd.gs.washington.edu/snv), MutationTaster (http://www.mutationtaster.org/) and NMDEscPredictor (https://fursham-h.github.io/factR/reference/predictNMD.html). SWISS-MODEL (https://swissmodel.expasy.org/) was used to construct a 3D model of the STAG2 protein. Co-segregation analysis of the *STAG2* and *PKD1* variants was performed among family members using

Sanger sequencing, with primers designed to amplify the *STAG2* variant [NM_001042750.2:c.1775_1777del, p.(Pro592del)] and the *PKD1* variant [NM_001009944.3:c.8985delC, p.(Ser2996fs*78)]. PCR amplification was performed with Takara PrimeSTAR Max DNA Polymerase (Takara Biotechnology Co., Ltd.) using the following thermocycling conditions: Initial denaturation at 95˚C for 5 min; 35 cycles of denaturation at 95˚C for 3 sec, annealing at 60˚C for 30 sec and extension at 72˚C for 30 sec; and a final extension at 72˚C for 5 min. The primer sequences were as follows: *STAG2* forward, 5'-TTTCCCTAAATGCCTCACAGAA-3' and reverse, 5'-AGG TACAGTTGTGGGCATGA-3'; and *PKD1* forward, 5'-CTC TGAGACTGCGACATCCA-3' and reverse, 5'-CACAGG AAACACAAAGCGGA-3'. The pathogenicity of candidate variants was assessed according to the guidelines of the American College of Medical Genetics and Genomics (ACMG)/ Association for Molecular Pathology (AMP) and the ClinGen Sequence Variant Interpretation Working Group (19,20).

Case presentation

Patient characteristics. The proband (III.1), a 4-month-old female infant, was the first child of unrelated non-consanguineous Chinese parents (Fig. 1A). The patient was born full-term at 40 weeks of gestation by vaginal delivery with a normal birth weight (3.19 kg). The Apgar scores of the infant at 1, 5 and 10 min after birth were 9, 9 and 10, respectively (21). At the age of 4 months, the patient was admitted to the Department of Pediatric Neurology of Maternal and Child Health Hospital of Guangxi Zhuang Autonomous Region for seizures. The proband experienced the first generalized tonic-clonic seizure at 3 months and 21 days old, with a frequency of 1-2 seizures per day during the first 9 days. A 24-h ambulatory electroencephalogram was performed, and the results showed bilateral slow waves and spike-like slow waves in the frontal pole, occipital and temporal areas (data not shown due to the large size of the video). Global developmental delay was observed in the first 4 months of life, and the patient was unable to hold their head up or roll over. A physical examination revealed that the patient had mild short stature (60 cm, <-2 SD), hypotonia and dysmorphic features, including microcephaly (head circumference of 39 cm, <-1 SD), a narrow forehead, saddle nose, large ears, micrognathia, incomplete cleft palate and microstomia (Fig. 1B). Additional findings included spina bifida occulta and a duplication of the middle phalanx of the third finger on the left hand. The neurodevelopmental parameters of the infant were assessed using the Bayley Scales of Infant and Toddler Development, Third Edition at ~6 months of age, and the cognitive, motor and language developmental ages were equivalent to those at 3, 4 and 2 months, respectively (22). Therefore, the patient was diagnosed with MKMS. Renal ultrasound demonstrated increased renal echogenicity (Fig. S1A). Notably, the mother, aunt and grandmother of the patient were all diagnosed with PKD, although no other malformations were reported in the family history. The proband did not exhibit other symptoms of ADPKD beyond the increased echogenicity observed in the renal ultrasound. Additionally, the patient did not have hypertension, and both urinalysis and serum creatinine levels were within normal ranges. Brain magnetic resonance imaging was performed at 4 months of age, and the results were normal (Fig. S1B). Audiological evaluation revealed no hearing deficits, but a middle ear infection was detected. The 4-month-old infant's ear infection was managed with a 10-day course of high-dose amoxicillin at 80-90 mg/kg per day, divided into two oral doses (~40 mg/kg twice daily). The last follow-up of the child was in November 2025, at which time the patient was 1.5 years old and developing normally.

Genetic analysis. Trio-WES identified a novel *de novo* heterozygous in-frame variant in *STAG2* [NM_001042750.2: c.1775_1777del, p.(Pro592del)] and a novel heterozygous frameshift variant in *PKD1* [NM_001009944.3:c.8985delC, p.(Ser2996fs*78)] (Fig. 1C). Both variants were confirmed in the proband and the family members by Sanger sequencing. The *STAG2* variant [c.1775_1777del, p.(Pro592del)] was absent in the parents, aunt and grandmother, confirming its *de novo* origin. By contrast, the *PKD1* variant [c.8985delC, p.(Ser2996fs*78)] was identified in the mother, aunt and grandmother of the proband (Fig. 1C). To the best of our knowledge, these variants have not been reported previously and are not identified in public databases, including the Exome Sequencing Project (https://evs.gs.washington.edu/EVS/), Genome Aggregation Database (https://gnomad.broadinstitute.org/), 1000 Genomes Project (https://www.internationalgenome.org/data) and the Single Nucleotide Polymorphism database (http://www.ncbi.nlm.nih.gov/SNP/), as well as disease-related databases such as ClinVar (https://www.ncbi.nlm.nih.gov/clinvar/) and the Human Gene Mutation Database (http://www.hgmd.cf.ac.uk/ac/). To date, a total of 21 distinct STAG2 variants, including the one reported here, have been identified in patients with HPE13 or MKMS, distributed across the entire gene (Fig. 1D). The variant described in the present report falls within the HEAT_SCC3-SA domain. To further analyze the effect of the amino acid changes caused by the c.1775_1777del, p.(Pro592del) variant on the structure of the protein, the variant was modelled using the wild-type STAG2 crystal structure. Pro592 is located at a junction between multiple α-helices, where it may influence their stability and packing (Fig. 2A); however, Pro592del leads to structural defects, disrupting the formation of α-helices (Fig. 2B). Therefore, we hypothesize that the c.1775_1777del, p.(Pro592del) variant may lead to defective protein folding and ultimately reduced stability of STAG2. According to the ACMG/AMP guidelines, the variant c.1775_1777del is classified as likely pathogenic (PS2 + PM2_Supporting + PP3), while the c.8985delC variant is classified as pathogenic (PVS1 + PM2_Supporting + PP1 + PP4) (Table I).

Discussion

STAG2 has been identified as a causative gene associated with a spectrum of neurodevelopmental disorders, including microcephaly, microphthalmia, hearing loss, developmental delay, dysmorphic features, congenital heart defects and digital anomalies (4,5). The association between *STAG2* and neurodevelopmental disorders was initially established through the identification of copy number variants affecting this gene. In addition, this association has been corroborated by the identification of novel single nucleotide variants, which have provided deeper insights into the genetic architecture of *STAG2*-related disorders (4,5). At present, 19 *STAG2* variants have been

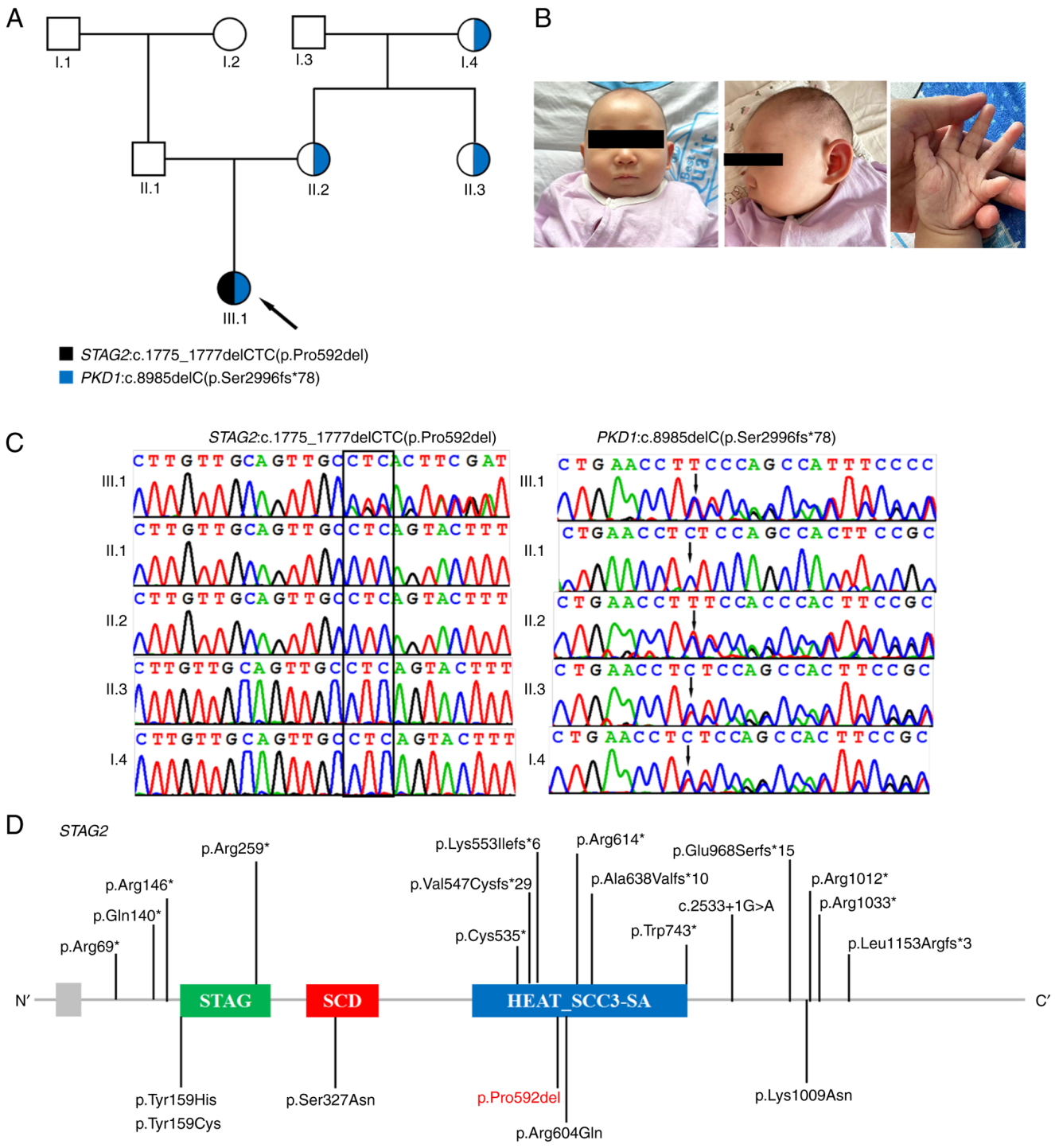

Figure 1. Clinical and genetic features. (A) Pedigree chart of the family of the proband with Mullegama-Klein-Martinez syndrome and familial polycystic kidney disease. The pedigree depicts the segregation of both the STAG2 (shown in black) and PKD1 (shown in blue) variants within the family. (B) Facial appearance of the proband (III-1) at the age of 4 months, showing microcephaly (head circumference of 39 cm, <-1 SD), narrow forehead, saddle nose, large ears, micrognathia and microstomia. (C) The Sanger sequencing chromatograms illustrate the presence of a novel heterozygous *STAG2* variant [NM_001042750.2:c.1775_1777del, p.(Pro592del)] and a novel heterozygous frameshift *PKD1* variant [NM_001009944.3: c.8985delC, p.(Ser2996fs*78)] in the proband. (D) The spectrum of *STAG2* pathogenic variants. The red variant is the novel variant identified in the present study. STAG, stromal antigen; SCD, stromalin conservative domain; HEAT_SCC3-SA, cohesin subunit SCC3/SA, HEAT-repeats domain.

identified in 25 patients with HPE13 or MKMS (4-13). In the current report, trio-based WES was performed, which identified a novel *de novo* heterozygous variant in the *STAG2* gene in a female Chinese infant. The patient exhibited a clinical phenotype consistent with *STAG2*-related disorders, including epilepsy, global developmental delay, short stature, hypotonia, dysmorphic features, incomplete cleft palate, micrognathia, spina bifida occulta and a duplication of the middle phalanx of the third finger on her left hand; therefore, the patient was diagnosed with MKMS.

The clinical features of the 26 reported patients with HPE13 or MKMS, including the patient in the current report,

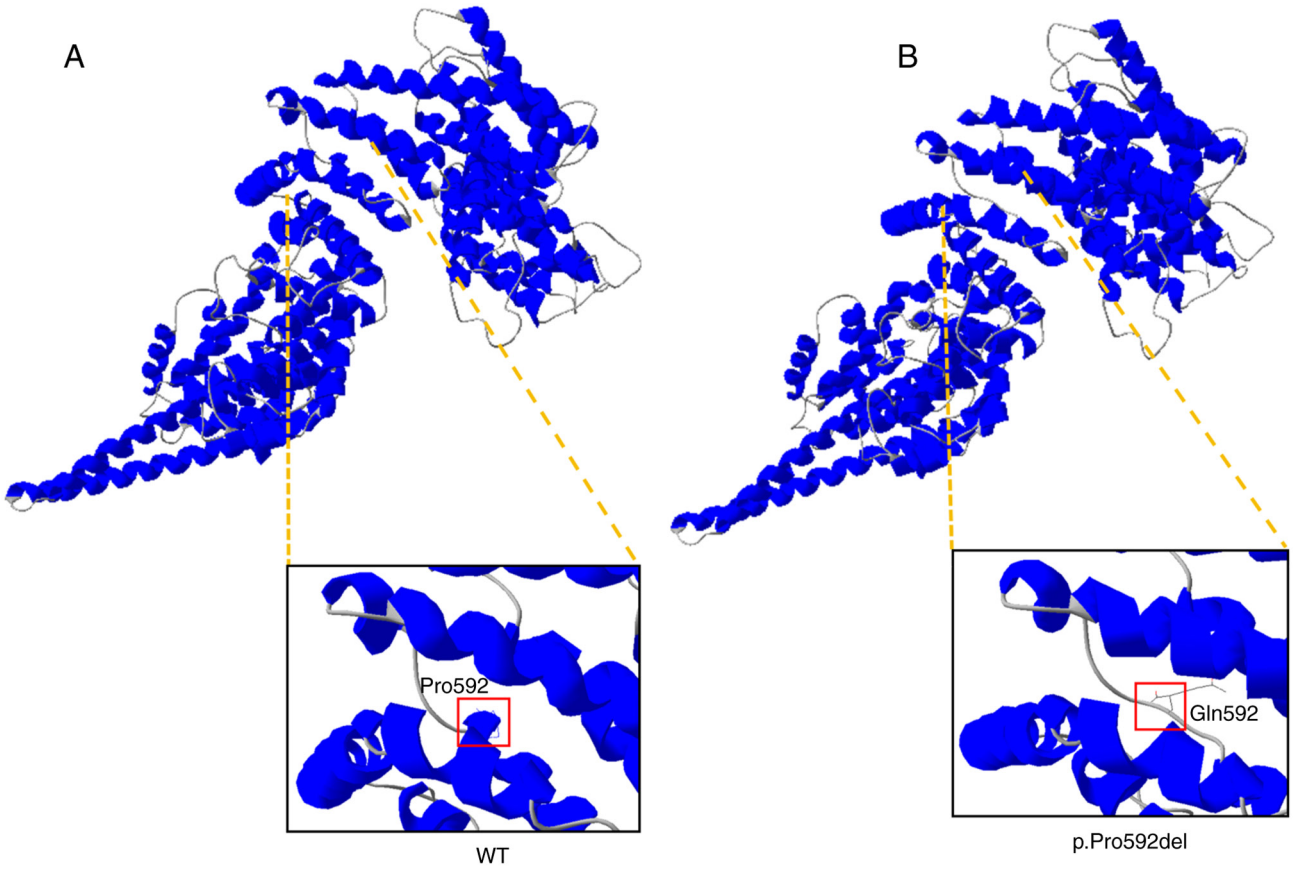

Figure 2. Three-dimensional molecular structure modeling of the STAG2 protein. (A) The crystal structure of the WT STAG2 shows that the Pro592 residue is located in the region composed of α-helices. (B) The Pro592del variant results in the disruption of α-helices. WT, wild-type; STAG2, stromal antigen 2.

are summarized in Table II. Phenotypic analysis of these patients revealed marked heterogeneity in the clinical features associated with pathogenic or likely pathogenic variants of the *STAG2* gene; however, certain common features were identified in >50% of cases. All patients with available data exhibited developmental abnormalities of varying severity across multiple domains. Intellectual disability or developmental delay was observed in all patients with available data (20/20), ranging from mild to severe. Pathogenic variants in the *STAG2* gene are associated with a spectrum of brain abnormalities. Brain anomalies were observed in almost all patients (15/17), and included microcephaly, delayed or incomplete myelination, myelin hypotrophy, agenesis or dysgenesis of the corpus callosum, white matter hypoplasia, holoprosencephaly and atelencephaly. Among these, holoprosencephaly (9/19) was the most frequently reported, whereas alobar holoprosencephaly represented the most severe manifestation. In the present patient, however, no brain malformations were observed at 4 months of age. Additionally, dysmorphic facial features were present in nearly all cases (19/21); individuals with MKMS typically exhibit characteristic facial dysmorphisms, including a broad forehead, low-set ears, a short and broad nose, a shallow philtrum, cleft lip/palate, a small mouth with thin lips and a small, receding chin (4,13). Ocular anomalies such as hypertelorism, hypotelorism, ptosis and epicanthal folds, as well as facial asymmetry, are also commonly observed. By contrast, patients with X-linked HPE13 often present with midline facial defects, such as a single central incisor, a flat nasal bridge and a proboscis (10). Ocular and eyelid abnormalities, including microphthalmia, anophthalmia, colobomas, ptosis and ankyloblepharon, are frequently noted, alongside oral and mandibular anomalies such as microstomia, macroglossia, cleft lip/palate and micrognathia. Dysmorphic features were shared in both conditions. The present patient also exhibited mild dysmorphic features including mild microcephaly, narrow forehead, saddle nose, large ears, micrognathia, incomplete cleft palate and microstomia. Thoracic vertebra abnormalities were observed in more than two-thirds (11/14) of the patients, primarily affecting the thoracic spine; these included hemivertebrae, butterfly vertebrae, scoliosis, spina bifida and fused ribs. Other skeletal anomalies involved left hip dysplasia, broad hands and feet and hyperextensibility of the hand and foot joints. The present patient also presented with spina bifida occulta accompanied by a novel clinical manifestation of middle phalanx duplication in the third digit of the left hand. Congenital cardiac malformations were also common (10/15), with a spectrum of anomalies ranging from patent foramen ovale to severe dextroposition of the heart and aortic valve atresia; notably, the present patient had no cardiac problems. Additional dysmorphic features included seizures, left facial palsy, mild left pelviectasis, sacral dimple, congenital dislocation of the hip, gastroesophageal reflux, hypotonia, pulmonary hypoplasia, single kidney, hearing loss, polycystic kidney, duodenal atresia and left-sided diaphragmatic hernia. These findings highlight the broad phenotypic spectrum associated with *STAG2* gene

Table I. Predicted pathogenicity of *STAG2* and *PKD1* variants.

Gene	Reference allele (GRCh38)	Variant	Inheritance	Variant Taster	NMDEscPredictor	PolyPhen-2	SIFT	CADD	ACMG/AMP guidelines
STAG2 (NM_001042750.2)	ChrX:124063159_124063161	c.1775_1777del, p.(Pro592del)	DNV	D	NA	NA	NA	NA	LP (PS2+PM2_ Supporting+PP3)
PKD1 (NM_001009944.3)	Chr16:2102597	c.8985delC, p.(Ser2996fs*78)	Maternal	D	Causes NMD	NA	NA	NA	P (PVS1+PM2_Supporting+PP1+PP4)

DNV, *de novo* variant; D, deleterious or damaging; NMD, nonsense-mediated mRNA decay; NA, not available; SIFT, Sorting Intolerant From Tolerant; CADD, Combined Annotation Dependent Depletion; P, pathogenic; LP, likely pathogenic; ACMG/AMP, American College of Medical Genetics and Genomics/Association for Molecular Pathology.

variants and underscore the importance of a comprehensive clinical evaluation in patients with these conditions. Further studies are needed to elucidate the underlying mechanisms and improve diagnostic and therapeutic approaches.

To date, only 26 affected individuals (including the present case) have been reported with *STAG2* variants, including five missense variants, one in-frame deletion (present case), eight nonsense variants, five frameshift variants and one splice variant (4-13). Notably, a distinct pattern emerged upon further analysis of these cases; all male patients (8/8) harbored hemizygous missense variants, whereas nearly all female patients (16/18) carried heterozygous null variants. A study by Cheng *et al* (23) showed that *Stag2* knockout mouse embryos displayed severe developmental defects and underwent necrosis at day E11.5, whereas conditional knockout mice with *Stag2* deletion in the nervous system exhibited growth retardation, neurological defects and early death. These results suggest that a hemizygous deletion of the *STAG2* gene may lead to severe phenotypes and could potentially cause embryonic lethality, thereby preventing the generation of male individuals with null variants. In addition, the present findings suggested that female patients with truncating variants exhibit a higher incidence of congenital malformations, such as brain malformations, cleft lip and palate, congenital heart disease, thoracic spine anomalies and epileptic seizures, compared with male patients with missense variants (Table III). These observations are likely driven by the greater pathogenic potential of truncating variants relative to missense variants, rather than by sex differences. Specifically, null variants typically result in a complete loss of function of the STAG2 protein, leading to more profound disruptions in cellular processes. By contrast, missense variants may retain partial protein function, potentially explaining the milder phenotypic manifestations observed in these cases. However, the precise mechanisms underlying these observations remain unclear and warrant further investigation through more comprehensive studies.

In the present study, the proband was also considered to have PKD. A renal ultrasound conducted at the age of 4 months revealed enhanced renal echogenicity. Furthermore, whole-exome sequencing in the proband identified pathogenic variants in the *PKD1* gene. A familial investigation further indicated that the mother, aunt and grandmother of the proband had previously been diagnosed with PKD. ADPKD is a common genetic renal disorder with an estimated worldwide incidence of 1:1,000. ADPKD is frequently associated with progressive renal failure (18), and variants in the *PKD1* gene are responsible for ~85% of ADPKD cases. Trio-WES analysis identified a heterozygous pathogenic variant [c.8985delC, p.(Ser2996fs*78)] in exon 25 of the *PKD1* gene in both the proband and the mother. Further validation in other family members by Sanger sequencing confirmed that this heterozygous variant was also detected in the affected aunt and grandmother of the patient, but it was not detected in other unaffected family members. There was co-segregation of the variant with the disease phenotype in this family. The novel frameshift variant was predicted to be disease-causing by MutationTaster, resulting in a premature termination codon or a translational frameshift, leading to the production of a truncated protein and markedly reduced

Table II. Clinical features of patients with *STAG2* variants.

Patient[a]	Sex	*STAG2* variants	Inheritance	ID/DD	Brain abnormalities	Micro-cephaly	Dysmorphic features and malfor-mations	Cleft lip/ palate	Congenital heart defects	Thoracic vertebra anomalies	Seizures	Other features	(Refs.)
1	M	c.3027A>T, p.(Lys1009Asn)	*De novo*	+	-	+	+	-	-	-	-	Polycystic kidney	(4)
One family (5 patients)	All M	c.980G>A, p.(Ser327Asn)	Maternally	5/5	NA	0/5	5/5	1/5	NA	NA	0/5	NA	(5)
7	F	c.3097C>T, p.(Arg1033*)	*De novo*	NA	HPE	NA	NA	+	Left heart hypoplasia	NA	-	NA	(6)
8	F	c.2229G>A, p.(Trp743*)	*De novo*	+	White matter hypoplasia	-	+	+	-	Hemivertebra	+	Amblyopia	
9	F	c.205C>T, p.(Arg69*)	*De novo*	+	HCC, subarachnoid cyst, subgaleal	+	+	+	VSD	Scoliosis, hemivertebra, butterfly vertebra	-	Left facial palsy, mild left pelviectasis	(7)
10	F	c.1913_1922del, p.(Ala638Valfs*10)	*De novo*	NA	NA	NA	NA	NA	NA	NA	NA	NA	
11	F	c.1840C>T, p.(Arg614*)	*De novo*	+	Cystic pituitary lesion	+	NA	NA	NA	Scoliosis	-	Sacral dimple, CDH	(8)
12	F	c.418C>T, p.(Gln140*)	*De novo*	+	NA	-	+	-	Left heart hypoplasia, VSD, CA	Scoliosis, rib fusion, verte-bral clefts	+	Gastroesophageal reflux, CDH	
13	F	c.1605T>A, p.(Cys535*)	*De novo*	+	NA	+	+	-	NA	Scoliosis, rib fusion	+	Hypotonia	
14	F	c.1658_1660delinsT, p.(Lys553Ilefs*6)	*De novo*	+	HPE (microform)	+	+	-	NA	Scoliosis, rib fusion	+	Hypotonia	(9)
15	F	c.1811G>A, p.(Arg604Gln)	*De novo*	+	NA	+	+	NA	-	Vertebral clefts	-	Gastroesophageal reflux, CDH, pulmonary hypoplasia	
16	M	c.476A>G, p.(Tyr159Cys)	*De novo*	+	Ectopic posterior pituitary, short pituitary stalk	-	+	+	Minimal PFO	Scoliosis	-	Single kidney, hypotonia	
17	F	c.205C>T, p.(Arg69*)	*De novo*	+	HPE (semi-lobar)	+	+	+	PFO, PDA	-	-	NA	(10)
18	F	c.436C>T, p.(Arg146*)	NA	NA	HPE (alobar)	+	+	-	VSD	Hemivertebra	-	Duodenal atresia	
19	F	c.775C>T, p.(Arg259*)	*De novo*	+	HPE (septo-optic dysplasia)	-	-	-	VSD	NA	-	Left hip dysplasia, bilateral optic nerve hypoplasia	

Table II. Continued.

Patient[a]	Sex	*STAG2* variants	Inheritance	ID/DD	Brain abnormalities	Micro-cephaly	Dysmorphic features and malfor-mations	Cleft lip/ palate	Congenital heart defects	Thoracic vertebra anomalies	Seizures	Other features	(Refs.)
20	F	c.3034C>T, p.(Arg1012*)	*De novo*	NA	HPE (alobar)	+	+	+	NA	Spina bifida	-	Gastroesophageal reflux	
21	F	c.2898_2899del, p.(Glu968Serfs*15)	*De novo*	+	HPE (microform)	+	NA	NA	-	NA	-	NA	
22	F	c.2533+1G>A	Maternally	NA	HPE (semi-lobar)	+	-	-	Left heart hypoplasia, DORV	NA	-	Hypotonia	
23	F	c.1639delG, p.(Val547Cysfs*29)	*De novo*	+	+	NA	+	NA	NA	NA	+	Hearing loss	(11)
24	F	c. 3458_3459delTT, p.(Leu1153Argfs*3)	*De novo*	NA	Dandy-Walker malformation	-	NA	-	Dextrocardia, CA, VSD	NA	-	CDH	(12)
25	M	c.475T>C, p.(Tyr159His)	Maternally	+	HPE, PMG, HCC	-	+	-	PFO	-	+	Hands and feet as well as fingers and toes were broad, with soft dorsal surfaces; the nails were deeply inserted and the joints of the hands and feet were hyperextensible	(13)
26	F	c.1775_1777delCTC, p.(Pro592del)	*De novo*	+	-	+	+	+	-	Spina bifida	+	Polycystic kidney, hypotonia	Present case
Total	M=8, F=18	Frameshift=5, Splicing=1, Nonsense=8, In-frame deletion=1, Missense=5		20/20	15/17	12/23	19/21	8/21	10/15	11/14	7/25		

[a]All patients were unrelated, except for patients 2-6, who were from the same family. The total row shows the total out of the number of cases with available clinical information. ID, intellectual disability; DD, developmental delay; F, female; M, male; NA, not available; HPE, holoprosencephaly; HCC, hypoplastic corpus callosum; PMG, polymicrogyria; VSD, ventricular septal defect; CDH, congenital diaphragmatic hernia; CA, coarctation of the aorta; PFO, patent foramen ovale; PDA, patent ductus arteriosus; DORV, double outlet right ventricle; +, yes; -, no.

Table III. Comparison of the effects of sex and variant type on clinical manifestations.

Clinical manifestation	Male patients with missense variants, n (%)	Female patients with truncating variants[a], n (%)	Total, n (%)
DD/ID	8/8 (100.00)	10/10 (100.00)	18/18 (100.00)
Microcephaly	1/8 (12.50)	9/13 (69.23)	10/21 (47.62)
Brain abnormalities	2/3 (66.67)	13/13 (100.00)	15/16 (93.75)
Dysmorphic features	8/8 (100.00)	9/11 (81.82)	17/19 (89.47)
Cleft lip/palate	2/8 (25.00)	5/12 (41.67)	7/20 (35.00)
Congenital heart defects	2/3 (66.67)	8/10 (80.00)	10/13 (76.92)
Thoracic vertebra anomalies	1/3 (33.33)	8/9 (88.89)	9/12 (75.00)
Seizures	1/8 (12.50)	5/15 (33.33)	6/23 (26.09)

[a]All frameshift, nonsense, start-loss and splice site variants were considered to be truncating variants. The total column shows the total out of the number of cases with available clinical information. ID, intellectual disability; DD, developmental delay.

mRNA levels due to nonsense-mediated mRNA decay. Consistent with the ACMG/AMP guidelines, this frameshift variant was classified as pathogenic, with the evidence criteria PVS1, PM2_supporting, PP1 and PP4. This finding confirmed that *PKD1* defects are likely to be the cause of PKD in this family. ADPKD is characterized by age-dependent and progressive clinical manifestations, usually becoming apparent in adulthood (18). While the proband, who was only 4 months old, had not shown typical PKD, these symptoms are expected to become more evident as the proband grows older. Therefore, a long-term follow-up plan needs to be established for this patient, with regular monitoring of renal ultrasound, glomerular filtration rate and urinary protein levels, to detect renal structural or functional abnormalities at an early stage and intervene in a timely manner. Notably, studies by Mullegama *et al* (4) and Yuan *et al* (9) reported two patients with *STAG2* variants who exhibited distinct renal anomalies, one presented with polycystic kidneys, while the other had a solitary kidney; however, genetic testing in these cases did not identify variants associated with PKD or renal dysplasia. Although no definitive studies have yet explored the specific role of STAG2 in kidney development, its widespread expression in various tissues, including the kidneys, and its critical role in cell proliferation, differentiation and gene regulation suggest that STAG2 may influence kidney development (5,7-8,10,24). For instance, in renal cancer tissues, the expression level of *STAG2* is markedly reduced, and its function is closely associated with cell proliferation and migratory capacity, indicating a potential role in the normal physiological processes of kidney cells (23). Additionally, while STAG2 and polycystin-1 are involved in different biological pathways, their functions may be interconnected at the cellular level. For instance, abnormalities in cell division and proliferation caused by *STAG2* mutations may indirectly affect kidney development or tissue homeostasis, thereby potentially influencing the manifestation of symptoms associated with polycystin-1; however, there is currently no direct evidence to suggest a clear molecular interaction between STAG2 and polycystin-1. In the present report, although pathogenic variants in the *PKD1* gene were detected in the patients, it cannot be excluded that *STAG2* gene variants may be associated with renal abnormalities. Furthermore, to accurately assess the role of STAG2 in kidney development, its potential interaction with polycystin-1 and the impact of *STAG2* variants on related diseases, further functional studies involving larger patient cohorts are required.

In conclusion, in the present study, a novel *de novo* *STAG2* variant was identified in a Chinese female infant with MKMS, expanding the clinical and genetic spectrum of *STAG2*-related disorders. Phenotypic analysis of additional 25 patients revealed marked heterogeneity; however, common features included intellectual disability, brain abnormalities, dysmorphic features and skeletal anomalies. Notably, loss-of-function variants were associated with more severe phenotypes compared with missense or in-frame variants, likely due to the complete loss of *STAG2* protein function. Additionally, a sex-biased distribution of variant types was observed, in which male patients predominantly harbored hemizygous missense variants, whereas female patients typically harbored heterozygous null variants. This pattern suggests potential sex-biased differences in disease severity, possibly influenced by X-chromosome inactivation or residual protein function in male patients. A pathogenic *PKD1* variant was also identified in the present patient, providing an independent explanation for the observed renal abnormalities. However, it is noteworthy that renal anomalies, including cystic dysplasia and renal hypoplasia, have also been reported in other *STAG2* variant carriers without concurrent *PKD1* variants or other identified nephropathy-associated genetic alterations. This phenotypic overlap suggests a potential pleiotropic role of *STAG2* in renal organogenesis. Nevertheless, the mechanistic relationship between *STAG2* variants and renal pathology remains poorly understood. In summary, the present findings emphasized the importance of genetic testing in diagnosing *STAG2*-related disorders. Future research should prioritize functional studies in larger cohorts to elucidate the molecular mechanisms of *STAG2* and its potential role in renal development. Such insights are critical for developing targeted therapies and improving the clinical management of patients with *STAG2*-related conditions.

Acknowledgements

Not applicable.

Funding

The present study was funded by the Health Department of Guangxi Province (grant nos. Z-A20220256, Z20190311 and Z20210309).

Availability of data and materials

The sequencing data generated in the present study may be found in the Sequence Read Archive database under accession number PRJNA1321735 or at the following URL: https://www.ncbi.nlm.nih.gov/sra/PRJNA1321735. The other data generated in the present study may be requested from the corresponding author.

Authors' contributions

QY and JL designed the study and drafted the manuscript. QiaZ, SheY, XZ, YR, SZ, ShaY, QinZ and ZQ collected the patients' clinical information and analyzed the WES data. QY and QiaZ revised the manuscript. All authors contributed to the coordination of the study and revised the manuscript. QY and JL confirm the authenticity of all the raw data. All authors read and approved the final version of the manuscript.

Ethics approval and consent to participate

The present study, involving the use of genetic testing for diagnosis, was approved by the Ethics Committee of Maternal and Child Health Hospital of Guangxi Zhuang Autonomous Region (approval no. METc 2017-2-11), and adhered to the principles of The Declaration of Helsinki. Written informed consent for genetic testing was obtained from the parents of the affected individual and the other relatives examined.

Patient consent for publication

Written informed consent was obtained from all adult patients and the parents of the minor individual for the publication of any potentially identifiable images or data included in this article.

Competing interests

The authors declare that they have competing interests.

References

1. Losada A: Cohesin in cancer: Chromosome segregation and beyond. Nat Rev Cancer 14: 389-393, 2014.
2. Musio A, Selicorni A, Focarelli ML, Gervasini C, Milani D, Russo S, Vezzoni P and Larizza L: X-linked cornelia de Lange syndrome owing to SMC1L1 variants. Nat Genet 38: 528-530, 2006.
3. Solomon DA, Kim T, Diaz-Martinez LA, Fair J, Elkahloun AG, Harris BT, Toretsky JA, Rosenberg SA, Shukla N, Ladanyi M, *et al*: Variantal inactivation of STAG2 causes aneuploidy in human cancer. Science 333: 1039-1043, 2011.
4. Mullegama SV, Klein SD, Mulatinho MV, Senaratne TN, Singh K; UCLA Clinical Genomics Center; Nguyen DC, Gallant NM, Strom SP, Ghahremani S, *et al*: De novo loss-of-function variants in STAG2 are associated with developmental delay, microcephaly, and congenital anomalies. Am J Med Genet A 173: 1319-1327, 2017.
5. Soardi FC, Machado-Silva A, Linhares ND, Zheng G, Qu Q, Pena HB, Martins TMM, Vieira HGS, Pereira NB, Melo-Minardi RC, *et al*: Familial a*STAG2* germline variant defines a new human cohesinopathy. NPJ Genom Med 2: 7, 2017.
6. Aoi H, Lei M, Mizuguchi T, Nishioka N, Goto T, Miyama S, Suzuki T, Iwama K, Uchiyama Y, Mitsuhashi S, *et al*: Nonsense variants of *STAG2* result in distinct congenital anomalies. Hum Genome Var 7: 26, 2020.
7. Mondal G, Stevers M, Goode B, Ashworth A and Solomon DA: A requirement for STAG2 in replication fork progression creates a targetable synthetic lethality in cohesin-mutant cancers. Nat Commun 10: 1686, 2019.
8. Yu L, Sawle AD, Wynn J, Aspelund G, Stolar CJ, Arkovitz MS, Potoka D, Azarow KS, Mychaliska GB, Shen Y, *et al*: Increased burden of de novo predicted deleterious variants in complex congenital diaphragmatic hernia. Hum Mol Genet 24: 4764-4773, 2015.
9. Yuan B, Neira J, Pehlivan D, Santiago-Sim T, Song X, Rosenfeld J, Posey JE, Patel V, Jin W, Adam MP, *et al*: Clinical exome sequencing reveals locus heterogeneity and phenotypic variability of cohesinopathies. Genet Med 21: 663-675, 2019.
10. Kruszka P, Berger SI, Casa V, Dekker MR, Gaesser J, Weiss K, Martinez AF, Murdock DR, Louie RJ, Prijoles EJ, *et al*: Cohesin complex-associated holoprosencephaly. Brain 142: 2631-2643, 2019.
11. Epilepsy Genetics Initiative: The epilepsy genetics initiative: Systematic reanalysis of diagnostic exomes increases yield. Epilepsia 60: 797-806, 2019.
12. Provenzano A, La Barbera A, Lai F, Perra A, Farina A, Cariati E, Zuffardi O and Giglio S: Non-invasive detection of a de novo frameshift variant of *stag2* in a female fetus: Escape genes influence the manifestation of X-linked diseases in females. J Clin Med 11: 4182, 2022.
13. Freyberger F, Kokotović T, Krnjak G, Frković SH and Nagy V: Expanding the known phenotype of Mullegama-Klein-Martinez syndrome in male patients. Hum Genome Var 8: 37, 2021.
14. Harris PC and Torres VE: Polycystic kidney disease. Annu Rev Med 60: 321-337, 2009.
15. Hughes J, Ward CJ, Peral B, Aspinwall R, Clark K, San Millán JL, Gamble V and Harris PC: The polycystic kidney disease 1 (PKD1) gene encodes a novel protein with multiple cell recognition domains. Nat Genet 10: 151-160, 1995.
16. Qian F, Germino FJ, Cai Y, Zhang X, Somlo S and Germino GG: PKD1 interacts with PKD2 through a probable coiled-coil domain. Nat Genet 16: 179-183, 1997.
17. Grantham JJ, Mulamalla S and Swenson-Fields KI: Why kidneys fail in autosomal dominant polycystic kidney disease. Nat Rev Nephrol 7: 556-566, 2011.
18. Cornec-Le Gall E, Alam A and Perrone RD: Autosomal dominant polycystic kidney disease. Lancet 393: 919-935, 2019.
19. Richards S, Aziz N, Bale S, Bick D, Das S, Gastier-Foster J, Grody WW, Hegde M, Lyon E, Spector E, *et al*: ACMG Laboratory quality assurance committee. Standards and guidelines for the interpretation of sequence variants: A joint consensus recommendation of the American College of Medical genetics and genomics and the association for molecular pathology. Genet Med 17: 405-424, 2015.
20. Rivera-Muñoz EA, Milko LV, Harrison SM, Azzariti DR, Kurtz CL, Lee K, Mester JL, Weaver MA, Currey E, Craigen W, *et al*: ClinGen variant curation expert panel experiences and standardized processes for disease and gene-level specification of the ACMG/AMP guidelines for sequence variant interpretation. Hum Mutat 39: 1614-1622, 2018.
21. Apgar V: A proposal for a new method of evaluation of the newborn infant. Originally published in July 1953, volume 32, pages 250-259. Anesth Analg 120: 1056-1059, 2015.
22. Spencer-Smith MM, Spittle AJ, Lee KJ, Doyle LW and Anderson PJ: Bayley-III cognitive and language scales in preterm children. Pediatrics 135: e1258-e1265, 2015.
23. Cheng N, Li G, Kanchwala M, Evers BM, Xing C and Yu H: STAG2 promotes the myelination transcriptional program in oligodendrocytes. Elife 12: e77848, 2022.
24. Yu C, Dai D and Xie J: Molecular subtype classification of papillary renal cell cancer using miRNA expression. Onco Targets Ther 12: 2311-2322, 2019.